

Finite-time stable disturbance observer for unmanned aerial vehicles

Pradhyumn Bhale¹, Mrinal Kumar², Amit K. Sanyal¹

Abstract— This work provides a finite-time stable disturbance observer design for the discretized dynamics of an unmanned vehicle in three-dimensional translational and rotational motion. The dynamics of this vehicle is discretized using a Lie group variational integrator as a grey box dynamics model that also accounts for unknown additive disturbance force and torque. Therefore, the input-state dynamics is partly known. The unknown dynamics is lumped into a single disturbance force and a single disturbance torque, both of which are estimated using the disturbance observer we design. This disturbance observer is finite-time stable (FTS) and works like a real-time machine learning scheme for the unknown dynamics.

I. INTRODUCTION

In recent years, unmanned aerial vehicles (UAVs) have been increasingly used in several applications ranging from security and monitoring, infrastructure inspection, agriculture and wildland management to package delivery, remote sensing and underwater exploration. All these applications have challenges, mainly due to the presence of obstacles and turbulence induced by air flow around structures or regions. In particular, the flight of a UAV over a wildland fire is subjected to unsteady and turbulent airflow, higher temperatures and variable density of air in such regions. These effects affect the flight of the UAV, creating disturbances in the form of perturbations, and bring adverse effects in the control performance of these UAVs [?], [?]. Because of these disturbances, a major challenge is to develop a complete model of the dynamics of the UAV in real time. To add to it, as the complexity of the dynamic system increases, the difficulty in modeling uncertain dynamics increases.

This work adds a unique and valuable approach to the numerous approaches proposed in research on control and observer designs for uncertain systems over the last two decades. These approaches are quite varied and use techniques like neural nets, fuzzy logic, soft computing, as well as data-driven extensions of predictive control, to learn the uncertainties in the dynamics [?], [?], [?], [?], [?], [?], [?]. Other data-driven approaches that use disturbance or uncertainty observers have also been treated in [?], [?].

Disturbance observers [?], [?] (DO) are advantageous in the design of robust control. They are commonly used to estimate uncertainties in nonlinear systems as they are easy, intuitive and possess a simple structure. Their main role is to estimate the disturbance inputs (uncertainties) to the dynamics. This helps in creating a modular design of

controllers where an outer loop controller can be designed for the nominal plant and the disturbance estimate from the DO is used to compensate it [?]. In this regard, a disturbance observer has an advantage over other control methods like \mathcal{H}_∞ control, adaptive control, or sliding mode control. Also, it offers a much larger design freedom for the controller design that works in the outer-loop. DO-based techniques provide a feasible way to improve robustness and deal with disturbances or system uncertainties in real time.

It is of critical importance in applications of UAVs with disturbance forces and torques, to ensure nonlinearly stable and robust performance of the disturbance observer. Stability requires that the identified disturbance changes by a small amount with small changes to inputs and outputs. Robustness requires that bounded changes to the system lead to bounded changes in the identified disturbance dynamics. In DO designs for uncertain systems, lack of guaranteed stability is a major shortcoming. The main contribution of this paper is a finite-time stable DO design for stable and robust learning of unsteady and unknown inputs on UAV flight dynamics. This DO is also designed in discrete time, making it convenient for onboard computation and implementation. The finite-time stable disturbance observer (FTSDO) obtained here has a faster convergence rate and better disturbance rejection abilities than conventional nonlinear DO. It can be designed to converge in a finite-time period that is smaller than the settling time of the controller. Dynamic systems that have a finite settling-time are more robust to bounded changes to their dynamics than asymptotically stable systems [?], [?].

An important aspect of this formulation is that local coordinates or quaternions are not used to represent the attitude on $\text{SO}(3)$. The observer is constructed to be finite-time stable (FTS) on the space of rigid body motions, $\text{SE}(3)$ which is the semi-direct product of \mathbb{R}^3 and $\text{SO}(3)$ [?]. One adverse consequence of unstable estimation and control schemes is that, if they converge or settle, they end up taking longer to converge compared to stable schemes with the same initial conditions and same initial transient behavior [?], [?]. Attitude and pose observers and filtering schemes on $\text{SO}(3)$ and $\text{SE}(3)$ have been reported in, e.g., [?], [?], [?], [?], [?]. Prior work on observer design and estimation directly on the Lie groups of rigid body motions can be found in [?], [?], [?].

The DO approach follows from the recent work [?], which developed a finite-time stable disturbance observer in discrete-time for a generalized MIMO system represented by an ultra-local model [?]. Unlike prior work, here we treat the complete 6-DoF dynamics for a UAV on the Lie group of rigid body motions $\text{SE}(3)$, using a disturbance observer.

¹ Department of Mechanical and Aerospace Engineering, Syracuse University, Syracuse, NY, 13244, USA. pbhale, aksanyal@syr.edu

² Department of Mechanical and Aerospace Engineering, The Ohio State University, Columbus, OH, 43210, USA. kumar.672@osu.edu

Part of the dynamics model for the UAV is known and the unknown (disturbance) inputs are estimated by the disturbance observer; together they make up a grey box model for the input-state dynamics. All the unknown dynamics of the model are combined into two terms, the disturbance force and the disturbance torque. The discretization of the equations of motion in the tangent bundle of $SE(3)$ are carried out in the framework of discrete geometric mechanics, and the resulting discrete-time equations are in the form of a Lie group variational integrator (LGVI) [?], [?]. As they are known to preserve energy-momentum properties and the geometry of the Lie group without any need of local projections, LGVI schemes are ideal for this application [?].

A brief outline of this paper is given here. In Section ??, we give some preliminaries regarding rigid body motion. The discretization of the kinematics and dynamics are given in Section ?? using the discrete-time Lagrange d'Alembert principle. Section ?? covers the main results for designing a finite-time stable disturbance observer to estimate the unknown dynamics. Numerical simulation results based on a LGVI scheme for the observer discretization are demonstrated in Section ???. We conclude the paper, in Section ??, by summarizing the results and highlighting possible future research directions.

II. PRELIMINARIES

A. Lie Group of Rigid Body Motions $SE(3)$

The set of possible configurations for rigid body translations and rotation is the Lie group $SE(3)$. The group $SE(3)$ is the semi-direct product of \mathbb{R}^3 and the special orthogonal group of rigid body orientations $SO(3)$, i.e., $SE(3) = \mathbb{R}^3 \times SO(3)$. The configuration of a rigid body is given by its position vector from the origin of an inertial coordinate frame \mathcal{I} to the origin of a body-fixed coordinate frame \mathcal{B} denoted $b \in \mathbb{R}^3$, and its attitude described by the rotation matrix from body-fixed frame \mathcal{B} to the inertial frame \mathcal{I} denoted by $R \in SO(3)$.

The special orthogonal group of rigid body rotation, $SO(3)$ [?], is defined by:

$$SO(3) = \left\{ R \in \mathbb{R}^{3 \times 3}, R^T R = R R^T = I, \det(R) = 1 \right\}.$$

$SO(3) \subset \mathbb{R}^{3 \times 3}$ is a matrix Lie group under matrix multiplication. The Lie algebra (tangent space at identity) of $SO(3)$ is denoted $\mathfrak{so}(3)$ and defined as,

$$\begin{aligned} \mathfrak{so}(3) &= \left\{ S \in \mathbb{R}^{3 \times 3} \mid S + S^T = 0 \right\}, \\ S = s^\times &= \begin{bmatrix} 0 & -s_3 & s_2 \\ s_3 & 0 & -s_1 \\ -s_2 & s_1 & 0 \end{bmatrix}. \end{aligned}$$

Here $(\cdot)^\times : \mathbb{R}^3 \rightarrow \mathfrak{so}(3)$ denote the bijective map from three dimensional Euclidean space to $\mathfrak{so}(3)$. For a vector $s = [s_1 \ s_2 \ s_3]^T \in \mathbb{R}^3$, the matrix s^\times represents the vector cross product operator, that is $s \times r = s^\times r$, where $r \in \mathbb{R}^3$. The inverse of $(\cdot)^\times$ is denoted $\text{vex}(\cdot) : \mathfrak{so}(3) \rightarrow \mathbb{R}^3$, such that $\text{vex}(a^\times) = a$, for all $a^\times \in \mathfrak{so}(3)$. Together with the

position vector of the (center of mass) of the rigid body, its pose (position and orientation) is given by:

$$g = \begin{bmatrix} R & b \\ 0 & 1 \end{bmatrix} \in SE(3). \quad (1)$$

B. System Kinematics and Dynamics

The instantaneous pose (position and attitude) is compactly represented by $g = (b, R) \in SE(3)$. Denoting the time derivative by (\cdot) , the UAV's kinematics is given by:

$$\begin{cases} \dot{b} = v = R\nu, \\ \dot{R} = R\Omega^\times, \end{cases} \quad (2)$$

where $v \in \mathbb{R}^3$ and $\nu \in \mathbb{R}^3$ denote the translational velocity in frames \mathcal{I} and \mathcal{B} respectively, and $\Omega \in \mathbb{R}^3$ is the angular velocity in frame \mathcal{B} . The dynamics of a rotorcraft UAV with a body-fixed plane of rotors is given by:

$$\begin{cases} m\ddot{b} = m\dot{v} = (f^c R - mg)e_3 + \phi_d, \\ J\dot{\Omega} = \tau^c - \Omega^\times J\Omega + \tau^d, \end{cases} \quad (3)$$

where $e_3 = [0 \ 0 \ 1]^T$, $f^c \in \mathbb{R}$ is the scalar thrust force and $\tau^c \in \mathbb{R}^3$ is the control torque created by the rotors, g denotes the acceleration due to gravity and $m \in \mathbb{R}^+$ and $J = J^T \in \mathbb{R}^{3 \times 3}$ are the mass and inertia matrix of the UAV, respectively. The disturbance force and torque are denoted ϕ^d and τ^d respectively, which are mainly due to unsteady aerodynamics. The discretization of this model using an LGVI scheme is expressed in the next section.

III. PROBLEM FORMULATION FOR DISTURBANCE OBSERVER ON $SE(3)$

A. Discrete-time Dynamics:

Let f_k denote the discrete approximation to a continuous time-varying quantity f at time $t_k = t(k)$. Let us denote $h \neq 0$ as the fixed step size, i.e., $t_{k+1} - t_k = h$. A discrete Lagrangian \mathcal{L} is constructed to approximate a segment of the action integral and we construct \mathcal{F} to approximate a segment of the virtual work integral and then, the discrete dynamics is prescribed by the discrete Lagrange-d'Alembert principle:

$$\delta \sum_{k=0}^{N-1} \mathcal{L}_k + \sum_{k=0}^{N-1} \mathcal{F}_k = 0, \quad (4)$$

Define the matrix inner product as the trace pairing $\langle \cdot, \cdot \rangle$:

$$\langle A, B \rangle := \text{tr}(A^T B).$$

The discrete-Lagrangian is chosen as the approximation:

$$\begin{aligned} \mathcal{L}_k(b, \nu, R, \Omega) &= \frac{h}{2} \langle m\nu_k, \nu_k \rangle + \frac{h}{2} \langle J \frac{1}{h} (\exp(h\Omega_k^\times) - I), \\ &\quad \exp(h\Omega_k^\times) - I \rangle - \frac{h}{2} (\mathcal{U}(b_k, R_k) + \mathcal{U}(b_{k+1}, R_{k+1})), \end{aligned} \quad (5)$$

where J is the inertia matrix, m is the mass of the body and $\mathcal{U}(b, R) : SE(3) \rightarrow \mathbb{R}$ denotes the potential energy function, which for a UAV in flight is given by uniform gravity:

$$\mathcal{U}(b, R) := \mathcal{U}(b) = mg b^T e_3. \quad (6)$$

The infinitesimal variations are given by:

$$\begin{cases} \delta b_k = R_k \gamma_k, \\ \delta R_k = R_k \Sigma_k^\times, \\ \delta \exp(\Omega_k^\times) = -\Sigma_k^\times \exp(\Omega_k^\times) + \exp(\Omega_k^\times) \Sigma_{k+1}^\times, \\ \delta \nu_k = \frac{1}{h} R_k^T (\delta b_{k+1} - \delta b_k) - \Sigma_k^\times \nu_k, \end{cases} \quad (7)$$

where Σ and γ vanish at the end points but are otherwise arbitrary. For \mathcal{F} , we choose an approximation of the form:

$$\mathcal{F}_k = \frac{h}{2} \langle \tau_k^\times, \Sigma_{k+1}^\times \rangle + h \langle \psi_k, R_{k+1} \delta b_{k+1} \rangle, \quad (8)$$

where τ and ψ denote the nonconservative moments and forces, respectively. The discrete kinematic equations as a first order forward Euler discretization of eq. (??) gives:

$$\begin{cases} b_{k+1} = b_k + h R_k \nu_k, \\ R_{k+1} = R_k \exp(h \Omega_k^\times), \end{cases} \quad (9)$$

Using the discrete Lagrange d'Alembert principle in (??), we get the discretized dynamic equations as:

$$\begin{cases} m \nu_{k+1} = m F_k^T \nu_k + h(f_k^c - mg R_k^T) e_3 + h \phi_k^d, \\ J \Omega_{k+1} = h \tau_k^c + \exp(-h \Omega_k^\times) J \Omega_k + h \tau_k^d, \end{cases} \quad (10)$$

where $F_k = R_k^T R_{k+1}$ and the whole number subscript $k \in \mathbb{W}$ denotes time variable corresponding to sampling instant t_k . These equations are obtained in the form of a Lie group variational integrator, and the matrix exponential in (??) is evaluated using Rodrigues' formula for numerical efficiency:

$$\exp(h \Omega^\times) = I + \frac{\sin \|h \Omega\|}{\|h \Omega\|} (h \Omega^\times) + \frac{1 - \cos \|h \Omega\|}{\|h \Omega\|^2} (h \Omega^\times)^2. \quad (11)$$

For a more detailed use of the discrete Lagrange d'Alembert principle to get the dynamic equations of a rigid body, the reader is directed to the previous works [?], [?]. Some definitions and lemma are stated next.

Definition 1: Any real-valued function $f : \Omega \rightarrow \mathbb{R}$ is Hölder continuous with exponent $\alpha \in (0,1)$ if it satisfies:

$$|f(x) - f(y)| \leq C \|x - y\|^\alpha,$$

for all x and y in the domain of f .

Lemma 1: Consider a discrete-time system with outputs $s_k \in \mathbb{R}^p \rightarrow \mathbb{R}$ and let $V : \mathbb{R}^p \rightarrow \mathbb{R}$ be a corresponding positive definite (Lyapunov) function and denote $V_k := V(s_k)$. Let α be a constant in the open interval $]0,1[$ and $\eta \in \mathbb{R}^+$. Denote $\gamma_k := \gamma(V_k)$ where $\gamma : \mathbb{R}_0^+ \rightarrow \mathbb{R}_0^+$ is a positive definite function of V_k . Let γ_k satisfy the condition:

$$\gamma_k \geq \eta := \epsilon^{1-\alpha} \text{ for all } V_k \geq \epsilon. \quad (12)$$

for some constant $\epsilon \in \mathbb{R}^+$. Then, if V_k satisfies the relation:

$$V_{k+1} - V_k \leq -\gamma_k V_k^\alpha, \quad (13)$$

the discrete system is (Lyapunov) stable at $s = 0$ and s_k converges to $s = 0$ for $k > N$, where $N \in \mathbb{W}$ is finite.

Proof: The proof of this lemma is given in [?] and omitted here for brevity. ■

Lemma 2: A discrete-time Lyapunov function that satisfies inequality (??) is Hölder-continuous in discrete time.

Proof: The proof of this lemma is given in [?] and omitted here for brevity. ■

IV. FINITE-TIME STABLE OBSERVER DESIGN

Many formulations are available to estimate the states from measured outputs in the equations of motion (??). These can be used in conjunction with the disturbance observer presented here. In this work, we assume that reasonably accurate state estimate are available from a novel scheme like [?], [?]. Using this assumption, the estimators for the disturbance forces and torques can be written as:

$$\begin{cases} \phi_k^d = \frac{1}{h} (m(\hat{\nu}_{k+1} - F_k^T \nu_k) - h(f_k^c - mg R_k^T) e_3), \\ \tau_k^d = \frac{1}{h} (J \hat{\Omega}_{k+1} - h \tau_k^c - \exp(-h \Omega_k^\times) J \Omega_k). \end{cases} \quad (14)$$

The unknown disturbance inputs $\chi_k^d = (\phi_k^d, \tau_k^d) \in \mathbb{R}^6$ are learnt in real time according to the past input-output history using (??). Let us define the error in estimating χ_k^d as:

$$e_k^\chi := \hat{\chi}_k^d - \chi_k^d. \quad (15)$$

Also, the first order finite difference of the unknown dynamics, χ_k^d , is denoted as:

$$\Delta \chi_k := \chi_k^{(1)} = \chi_{k+1}^d - \chi_k^d \quad (16)$$

The disturbance estimate $\hat{\chi}_{k+1}^d$ can be obtained in real time from the following first order nonlinearly stable observer.

Theorem 1: The nonlinear observer for χ_k given by

$$\chi_{k+1}^d = \mathcal{D}(e_k^\chi) e_k^\chi + \chi_k^d, \quad (17)$$

where $\hat{\chi}_0^d = \chi_0^d$ is given and $\mathcal{D} : \mathbb{R}^+ \rightarrow \mathbb{R}$ is a Hölder-continuous function that is given by:

$$\mathcal{D}(e_k^\chi) = \frac{((e_k^\chi)^T e_k^\chi)^{1-1/r} - \lambda}{((e_k^\chi)^T e_k^\chi)^{1-1/r} + \lambda}, \quad (18)$$

and $\lambda > 0$ and $r \in (1, 2)$ are constants. This observer design leads to finite time stable convergence of the estimation error vector $e_k^\chi \in \mathbb{R}^6$ to a bounded neighborhood of $0 \in \mathbb{R}^6$, where bounds on the neighborhood are obtained from the bounds on ΔF_k .

Proof: Consider the discrete-time Lyapunov function

$$V_k^\chi := (e_k^\chi)^T e_k^\chi. \quad (19)$$

Taking the first order discrete-time difference of this Lyapunov function gives us:

$$\begin{aligned} V_{k+1}^\chi - V_k^\chi &= -\gamma_k^\chi (V_k^\chi)^{\frac{1}{r}}, \\ \text{where } \gamma_k^\chi &= (1 - (\mathcal{D}(e_k^\chi))^2) (V_k^\chi)^{1-\frac{1}{r}}. \end{aligned} \quad (20)$$

This implies that γ_k^χ is a positive definite function of $V_k^\chi = \|e_k^\chi\|^2$. Using (??) and (??), we can express γ_k^χ as a function of V_k^χ :

$$\gamma_k^\chi = 4\lambda \frac{(V_k^\chi)^{2-\frac{2}{r}}}{((V_k^\chi)^{1-\frac{1}{r}} + \lambda)^2}. \quad (21)$$

It can be inferred from (??) that $\gamma_k^\chi := \gamma(V_k^\chi)$ is a class- κ function of V_k^χ . Moreover, it can be verified that:

$$\implies V_N^\chi \leq \lambda^{\frac{1}{1-1/r}},$$

$$\implies \gamma_N^\chi \leq \lambda.$$

The last two results together imply that γ_k^χ satisfies the sufficient condition for finite-time stability of e_k^χ stated in Lemma 1. Now, consider the expression for e_{k+1}^χ given by

$$e_{k+1}^\chi = \mathcal{D}(e_k^\chi)e_k^\chi, \quad (22)$$

Using (??) and (??), the following discrete-time disturbance observer for χ_k^d is obtained:

$$\dot{\chi}_{k+1}^d = \mathcal{D}(e_k^\chi)e_k^\chi + \chi_{k+1}^d. \quad (23)$$

The above expression leads to a finite-time stable observer for the unknown dynamics that ensures that the estimation error e_k^χ converges to zero for $k > N$ where $N \in \mathbb{W}$ is finite. However, due to the causality of the dynamics, the value of χ_{k+1}^d is not available at time t_{k+1} , and it needs to be replaced by a known quantity. Consequently, χ_{k+1}^d is replaced by χ_k^d in (??) to obtain the first-order observer design given by (??).

The observer given by equation (??) is basically a first-order perturbation of the ideal FTS observer design for χ_k^d as given by (??). The first-order finite difference term $\Delta\chi_k$ is the source of the perturbation in this case. ■

Theorem 2: Consider the nonlinear observer law for the disturbance χ_k^d given by (??). Let the bound on the first order difference $\Delta\chi_k$ defined by (??) be given by:

$$\|\Delta\chi_k\| \leq B^\chi, \quad (24)$$

where $B^\chi \in \mathbb{R}^+$. Then, the observer estimation error e_k^χ is guaranteed to converge to the neighborhood given by:

$$N^\chi := \{e_k^\chi \in \mathbb{R}^n : \rho(e_k^\chi)\|e_k^\chi\| \leq B^\chi\}, \quad (25)$$

for finite $k > N$, $N \in \mathbb{W}$, where

$$\rho(e_k^\chi) := 1 + |\mathcal{D}(e_k^\chi)|. \quad (26)$$

Proof: Using the Lyapunov equation defined by (??) and the observer equation (??), we obtain

$$\begin{aligned} V_{k+1} - V_k &= ((\mathcal{D}(e_k^\chi))^2 - 1)(e_k^\chi)^T e_k^\chi - 2\mathcal{D}(e_k^\chi)\Delta\chi_k^T e_k^\chi \\ &\quad + \Delta\chi_k^T \Delta\chi_k, \end{aligned}$$

Using the bound on the value of $\|\Delta\chi_k\|$ given by (??), we can get an upper bound on the first difference of the Lyapunov function:

$$\Delta V_k^\chi \leq (\mathcal{D}^2 - 1)\|e_k^\chi\|^2 + 2|\mathcal{D}|B^\chi\|e_k^\chi\| + (B^\chi)^2, \quad (27)$$

where $\mathcal{D} := \mathcal{D}(e_k^\chi)$ for ease of notation. For large enough initial (transient) $\|e_k^\chi\|$, the right hand side of the inequality (??) is negative, which gives us the following condition:

$$(1 - \mathcal{D}^2)\|e_k^\chi\|^2 - 2|\mathcal{D}|B^\chi\|e_k^\chi\| - (B^\chi)^2 > 0, \quad (28)$$

The above equation (??) can be considered as a quadratic inequality expression in $\|e_k^\chi\|$ with coefficients that depend on e_k^χ . This leads to the condition,

$$(|\mathcal{D}(e_k^\chi)| + 1)\|e_k^\chi\| > B^\chi, \quad (29)$$

for real positive solutions of $\|e_k^\chi\|$ for which $\Delta V_k^\chi < 0$ is guaranteed. Note that $\mathcal{D}(e_k^\chi)$ is a monotonically increasing

function taking values in the range of $[-1, 1]$. The discrete Lyapunov function V_k^χ will decrease monotonically for $\|e_k^\chi\|$ large enough to satisfy inequality (??), which it will until a finite value of k , say $k = N$. Therefore, the observer error is guaranteed to converge to the neighborhood N^χ of the zero vector $\in \mathbb{R}^6$ given by equation (??) and will stay in this positively invariant neighborhood for $k > N$. ■

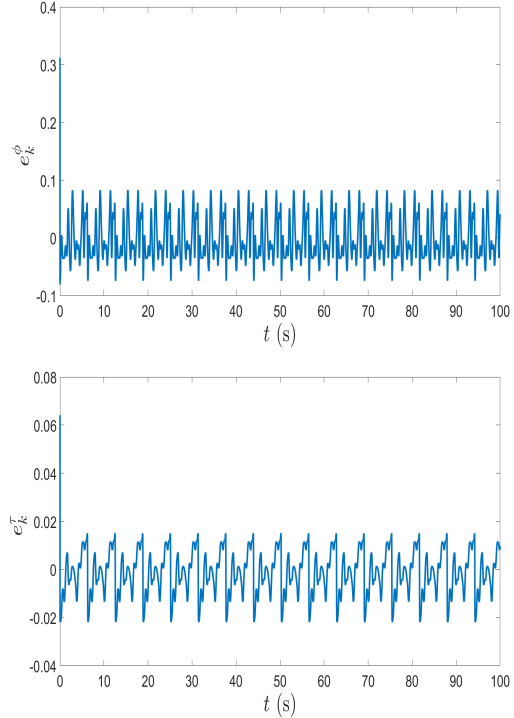


Fig. 1: Model estimation error for (a) disturbance force, and (b) disturbance torque, without noise

V. NUMERICAL SIMULATION

In this section, a comprehensive numerical simulation study for the FTS disturbance observer presented in Theorem 1 is carried out. The disturbance estimation error vector from this disturbance observer is shown to converge in finite-time to a bounded neighborhood of the zero vector $\in \mathbb{R}^6$ as given by Theorem 2.

A. Finite-time Convergence

Dynamic turbulent wind effects are difficult to model exactly, even with the use of detailed CFD analysis and simplifying assumptions for the wind fields. The uncertainties that exist in a realistic wind field contain a variety of different atmospheric sources like turbulence, vortex, gust and shear. Despite this, a combination of sinusoidal wave-forms are generally sufficient to capture the dominant characteristics that exist in a realistic wind field.

To this avail, the wind disturbance is simulated here as a combination of sinusoidal frequencies. To make the wind model more realistic and close to a real-world environment, lower frequency signals of relatively high amplitude are combined with higher frequency signals of relatively low

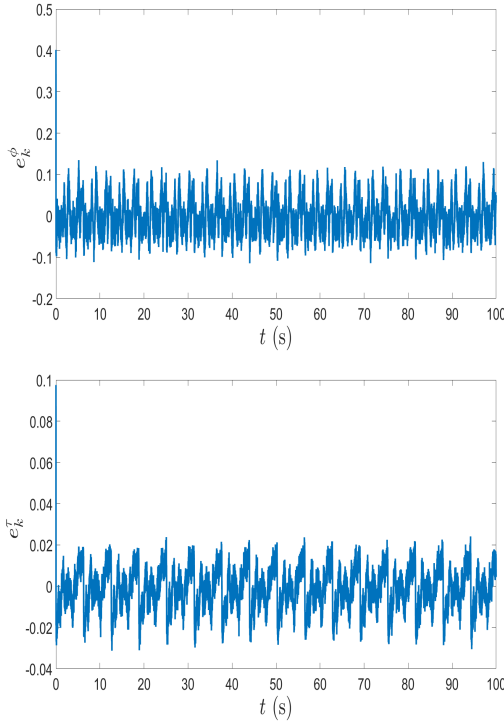


Fig. 2: Model estimation error for (a) disturbance force, and (b) disturbance torque, with noise

amplitude, with the frequencies being not more than 10 Hz. The total magnitude of the force and torque disturbance is of the order of $\sim 5\text{-}7$ N and $\sim 1\text{-}2$ N-m, respectively.

These disturbances are propagated through the system dynamics (??). In the simulation, the measurements are generated by numerically propagating the true discrete-time dynamics. For the results in this subsection, no (measurement) noise is added to the outputs and only the finite-time convergence of the disturbance estimates is examined. Output measurements are assumed at a constant rate of 50 Hz, i.e. sampling period $\Delta t = 0.02$ s. The unknown disturbance dynamics is obtained from the estimated outputs.

The first order finite-time stable observer stated in Theorem 1 is used for estimating the disturbance inputs. The Hölder-continuous function $\mathcal{D}(e_k^\chi)$ defined in (??) is used with the observer gains:

$$\lambda = 1.0, \text{ and } r = \frac{9}{7}.$$

Simulation results for the estimation error in estimating the unknown (disturbance) dynamics are depicted in Figure ???. The disturbance term $\chi_k^d \in \mathbb{R}^6$ comprises of two parts: the disturbance force $\Phi_k^d \in \mathbb{R}^3$, and the disturbance torque $\tau_k^d \in \mathbb{R}^3$. Figure ?? shows the estimation error in the magnitude of disturbance force $\|\Phi_k^d\|$ and disturbance torque $\|\tau_k^d\|$, respectively. It can be inferred from the plots that the disturbance estimation error vector settles down in a neighborhood of the zero vector in finite-time when the initial disturbance estimation error vector is outside this neighborhood. This validates the finite-time convergence of

the first-order nonlinear observer given by (??). This ideal scenario where the outputs do not have any measurement noise associated with them is not realistic and hence, robustness to output measurement noise is tested.

B. Robustness to measurement noise

Generally, the output states measured have additive measurement noise, which results in the calculated disturbance obtained from the input-output dynamics (as shown in (??)) being different from the actual disturbance inputs that are acting on the system dynamics. A robust disturbance observer will make the disturbance estimates converge to a bounded neighborhood in the presence of bounded measurement noise.

Here, simulations are carried out in a similar setting as the previous subsection. In this case, the measurements are generated by numerically propagating the true discrete-time dynamics and adding noise to the true outputs. The added noise signals are taken to be $\sim 2\%$ of the true output values which gives a realistic signal-to-noise ratio (SNR) of around 30 dB. This is representative of current off-the-shelf sensors that are used in the UAV industry.

Simulation results for the estimation error with added noise are depicted in Figure ???. It shows the estimation error in the magnitude of disturbance force $\|\Phi_k^d\|$ and disturbance torque $\|\tau_k^d\|$, respectively. The numerical results show good finite-time convergence of the disturbance estimation errors to a bounded neighborhood of the zero vector, further validating the robustness of the observer design.

C. Convergence bounds for the DO

Theorem 2 gives a bound for the observer estimation error which in turn is dependent on the bound on the first order finite difference of the unknown dynamics, χ_k^d . For the disturbance force Φ_k^d , the total magnitude is of the order of $\sim 5\text{-}7$ N and simulated measurements are taken at a constant rate of 50 Hz, as stated earlier. This gives a bound B^Φ for the first order difference of the disturbance force. Calculating the value of B^Φ and using (??) gives:

$$\|\Delta\Phi_k^d\| \leq 0.14, \quad (30)$$

From (??), we get:

$$\rho(e_k^\Phi)\|e_k^\Phi\| \leq 0.14, \quad (31)$$

Taking the maximum value of e_k^Φ and substituting it in the expression for $D(e_k^\Phi)$ given by (??), we get the value of $\rho(e_k^\Phi)$ from (??) as:

$$\rho(e_k^\Phi) \approx 1.5, \quad (32)$$

From (??) and (??), we get:

$$\|e_k^\Phi\| \leq .095, \quad (33)$$

For the disturbance torque, the total magnitude is of the order $\sim 1\text{-}2$ N-m and similarly, the bound for the first order difference of the disturbance torque can be given by:

$$\|\Delta\tau_k^d\| \leq 0.035, \quad (34)$$

Similarly, from (??) we get:

$$\rho(e_k^\tau) \|e_k^\tau\| \leq 0.035, \quad (35)$$

Following the same procedure as for the disturbance force earlier, we get:

$$\rho(e_k^\tau) \approx 1.7, \quad (36)$$

From (??) and (??), we get the bound for the estimation error for the magnitude of disturbance torque given as:

$$\|e_k^\tau\| \leq 0.021 \quad (37)$$

The bounds (??) and (??) on estimation errors in disturbance force and torque are satisfied by the plots in Fig. ??.

VI. CONCLUSION AND FUTURE WORKS

This research proposes a first order discrete-time disturbance observer for a rigid body with disturbance force and disturbance torque inputs. The observer design is shown to be nonlinearly stable and robust in estimating the disturbances in real-time. The observer design makes the estimation errors converge to a bounded neighborhood of zero errors. A comprehensive simulation study for the observer design is carried out for performance validation. In future work, asymptotically stable or finite-time stable control schemes will be designed to run in conjunction to formulate a unified data-driven robust feedback control scheme. Another future direction will be to obtain LGVI discretization schemes for the case of variable time step size. Another important future work will be the examination of the bounds on the estimation errors for the disturbance force and torque in the presence of measurement noise in the true outputs.

ACKNOWLEDGEMENT

The authors acknowledge support from the National Science Foundation award 2132799.